

Development of a Sensitive Immunochromatographic Method Using Lanthanide Fluorescent Microsphere for Rapid Serodiagnosis of COVID-19

Meng Feng, Jun Chen, Jingna Xun, Ruixue Dai, Wang Zhao, Hongzhou Lu, Jin Xu, Li Chen, Guodong Sui,* and Xunjia Cheng*



Cite This: <https://dx.doi.org/10.1021/acssensors.0c00927>



Read Online

ACCESS |



Metrics & More



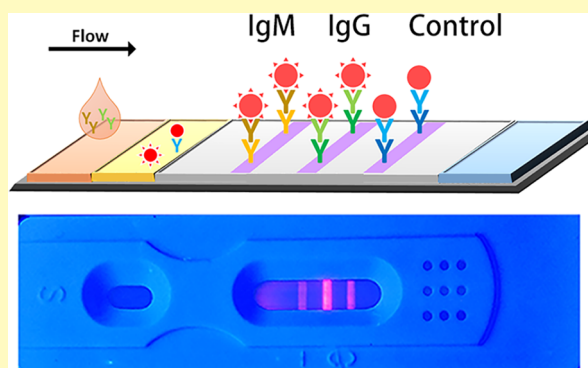
Article Recommendations



Supporting Information

ABSTRACT: The SARS-CoV-2 infection that caused the COVID-19 pandemic quickly spread worldwide within two months. Rapid diagnosis of the disease and isolation of patients are effective ways to prevent and control the spread of COVID-19. Therefore, a sensitive immunofluorescent assay method was developed for rapid detection of special IgM and IgG of COVID-19 in human serum within 10 min. The recombinant nucleocapsid protein of 2019 novel coronavirus was used as capture antigen. Lanthanide, Eu(III) fluorescent microsphere, was used to qualitatively/semiquantitatively determine the solid phase immunochromatographic assay. A total of 28 clinical positive and 77 negative serum or plasma samples were included in the test. Based on the analysis of serum or plasma from COVID-19 patients and healthy people, the sensitivity and specificity of the immunochromatographic assay were calculated as 98.72% and 100% (IgG), and 98.68% and 93.10% (IgM), respectively. The results demonstrated that rapid immunoassay has high sensitivity and specificity and was useful for rapid serodiagnosis of COVID-19.

KEYWORDS: SARS-CoV-2, serodiagnosis, immunochromatographic, fluorescent microsphere, nucleocapsid protein



Since December, 2019, a series of infectious disease outbreaks has swept the globe.¹ Subsequently, the viral genome was sequenced in a short time and the results suggested a novel type of human coronavirus named 2019 novel coronavirus (WHO officially named SARS-CoV-2).^{1,2} Before the outbreak of this novel coronavirus, there were two previous coronavirus infections in humans, the 2003 severe acute respiratory syndrome coronavirus (SARS-CoV) and 2012 Middle East respiratory syndrome coronavirus (MERS-CoV).^{3–5} The disease caused by SARS-CoV-2 infection was named COVID-19; it was a pandemic within two months in many countries of the world, rapidly becoming the biggest global public health problem in 2020.

Rapid diagnosis and isolation of patients is an effective way to prevent and control the spread of COVID-19. Currently, virus nucleic acid Real Time-PCR (RT-PCR), Reverse Transcription Loop-mediated isothermal amplification (RT-LAMP), and Computed Tomography (CT) imaging are being used for laboratory diagnosis of COVID-19.^{6–8} In China, the virus nucleic acid RT-PCR was first used, and then RT-LAMP test was used for its convenience. Typical pulmonary imaging changes in CT are an important reference for early diagnosis of COVID-19. However, about 20% of false negatives for nucleic acid test of COVID-19 were reported due to various factors,

such as easy degradation of RNA or deficiency of virus nucleic acid in respiratory secretion of patients.^{8,9} Therefore, other diagnostic methods have been urgently needed.

Different serological testing has been employed to detect certain viruses, including immunofluorescent assays, enzyme-linked immunosorbent assays, and immunochromatographic tests. ELISA- or chemiluminescent assay-based detection of coronavirus proteins was used to detect the presence of viral proteins in patient serum samples.^{10–12} A rapid and simple method for serodiagnosis of SARS-CoV-2 could help for disease diagnosis. Many studies in SARS infection indicated that IgM antibody could be detected in patient serum within 3–6 days, and then IgG would rise rapidly.^{13–15} The immunochromatographic method is regarded as a rapid and convenient method widely used in a variety of diseases, including infectious diseases.^{16,17} Its principle is simple and

Received: May 6, 2020

Accepted: July 14, 2020

Published: July 14, 2020

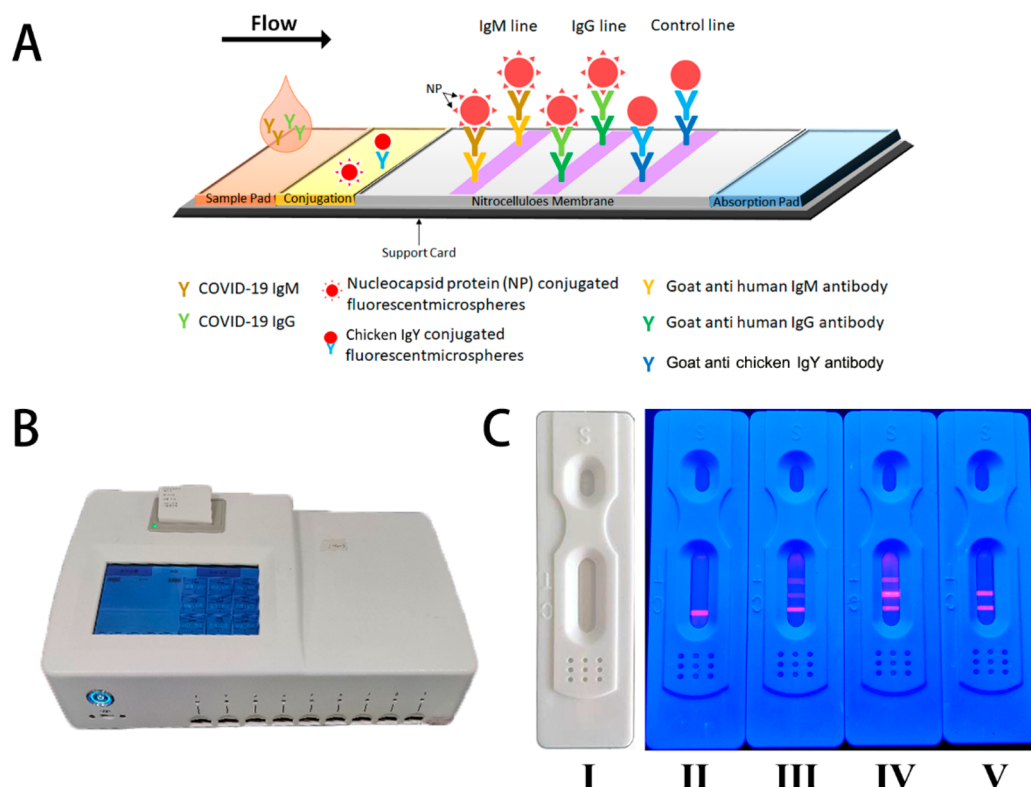


Figure 1. Schematic chart of SARS-CoV2 IgG/IgM rapid immunochromatographic assay. (A) Principle of detection of IgM and IgG antibodies to NP. (B) Immunochromatographic reader. The results of the value and chart could be displayed on liquid crystal display panel. (C) Representative photo for different patient serum testing results under UV lamp. Plastic cassette (I); no IgM and IgG (II); low concentration of IgM and IgG (III); high concentration of IgM and IgG (IV); high concentration of IgG and no IgM (V).

easily accepted by doctors; these advantages make it especially suitable for a serious epidemic situation. In the current study, a sensitive immunofluorescent assay method was developed for rapid detection of special IgM and IgG of COVID-19 in human serum or plasma within 10 min. Dozens of positive and negative serum or plasma samples were tested, and results demonstrated that the rapid immunoassay was successful and useful for rapid serodiagnosis of COVID-19. We hope this method can contribute to the control of the pandemic.

MATERIALS AND METHODS

In this study, 2 positive serum and 26 positive plasma samples were examined. These clinical samples tested positive for SARS-CoV-2 by RT-PCR using pharyngeal test paper as material in Shanghai CDC, China. 77 negative serum samples were collected from 2009 to 2018 and were stored at $-80\text{ }^{\circ}\text{C}$ before use.

All samples were anonymized. The Institutional Ethics Committees of Shanghai Public Health Clinical Center approved the study's protocol (ethics approval no. YJ-2020-S021-01) and School of Basic Medical Sciences, Fudan University (2018-Y022).

Recently, microspheres containing a fluorescent dye proved to have great advantages for antibody detection. In this study, we used lanthanide, Eu(III) fluorescent microsphere to detect SARS-CoV-2 specific IgM and IgG in serum from patients and then developed a new immunochromatographic method for rapid serodiagnosis.

A full length of nucleocapsid protein (NP) gene of SARS-CoV was cloned to pGEX-2T vector after codon optimization. Then recombinant NP with GST tag was prokaryotically expressed in BL21(DE3) *Escherichia coli* bacteria (Figure S1) as previously described.¹⁸ The NP was immobilized onto the polystyrene lanthanide Eu(III) fluorescent microspheres by carbodiimide coupling between the carboxylic groups of the microspheres and amine groups of the NP. The procedures were briefed in the following steps: First,

microspheres (3.125×10^6) were added into 250 μL buffer with 0.250 mL 0.1 M NaH_2PO_4 (pH 6.2) buffer and sonicated for 1 min. After centrifuge, the microspheres were added into 0.5 mL solution which contained *N*-hydroxysulfosuccinimide (2.5 mg) and *N*-(3-(dimethylamino)propyl)-*N*-ethylcarbodiimide (2.5 mg) for 20 min at room temperature. The phosphate buffered saline (PBS) (PH 7.4) was used to wash the microspheres twice. The activated microspheres were added into 0.5 mL PBS buffer containing 12.5 μg NP, and the whole mixture was rotated and incubated for 3 h at room temperature to complete the coupling process. Then, collected microspheres were washed by PBS buffer containing 0.05% NaN_3 and centrifuged. The microspheres were added into PBS containing 1.0% bovine serum albumin for 0.5 h to minimize the nonspecific binding. The NP-coupled fluorescent microsphere solution at concentration of $2.0 \times 10^6/\text{mL}$ was stored for further utilization.

The test strip consists of five parts, including the support card, sample pad, conjugate pad, nitrocellulose membrane, and absorbent pad (Figure 1A). The absorbent pad, sample pad, and membrane were assembled on a laminated membrane card. The anti-human-IgM, anti-human-IgG, and anti-chicken-IgY were sprayed onto the nitrocellulose membrane to form IgM (T2 line), IgG (T1 line), and control line (C line) using an XYZ3060 Dispense Platform, respectively. The conjugate pad was sprayed with mixture of NP conjugate fluorescent microspheres and chicken IgY conjugate fluorescent microspheres. The sample pad was pretreated with 3% bovine serum albumin containing 0.5% Tween-20 before use. Finally, the assembled sheet was cut into 4 mm strips and put into a plastic cassette. All the reagents and experiments were performed in accordance with the manufacturer's instructions.

The clinical samples were processed as follows: 2 μL of each sample (serum or plasma) was first diluted with 98 μL of PBS buffer (pH 7.4) (ratio of 1:50), and then 80 μL of diluted samples was taken and loaded to the testing well of the assembled cassette for diagnosis.

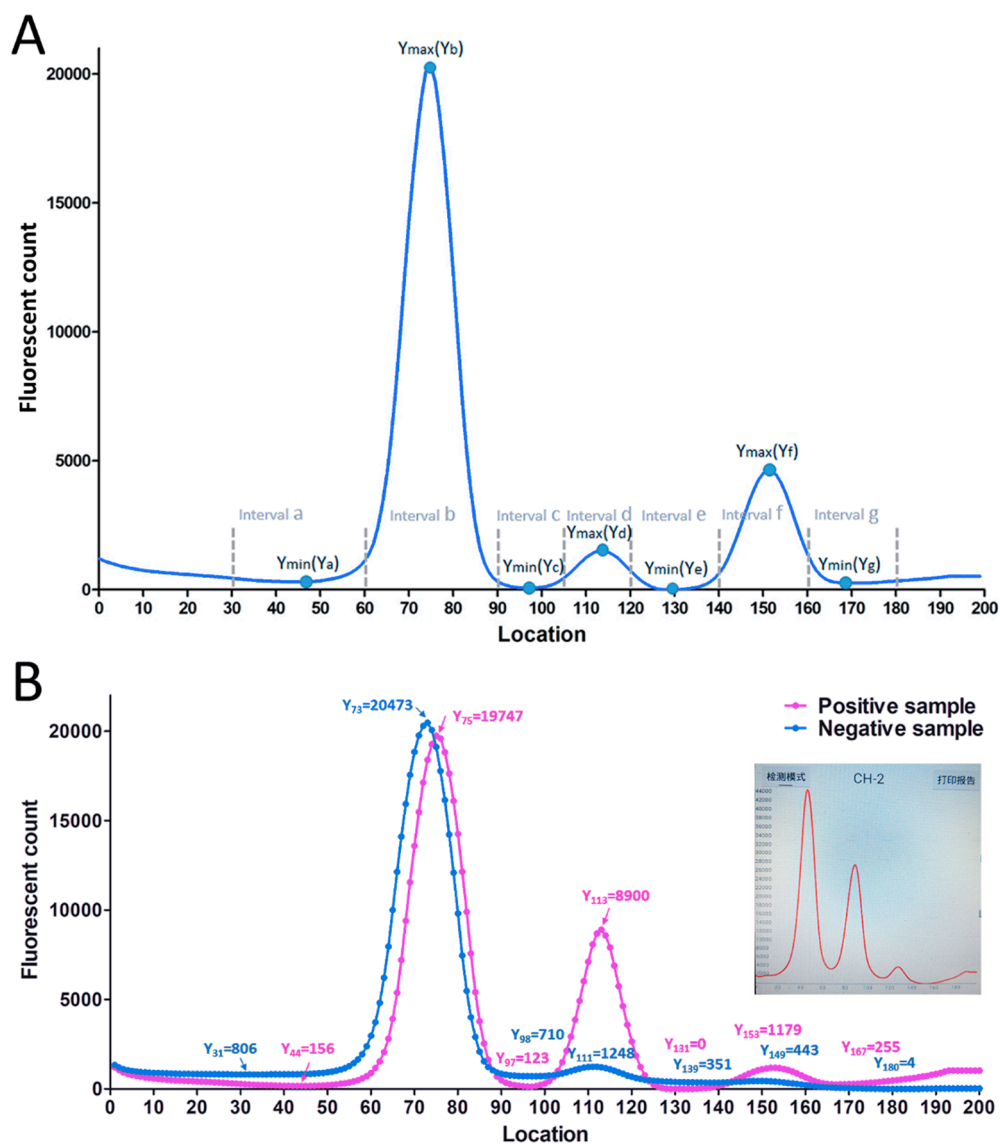


Figure 2. Scanning waveforms of fluorescence in immunochromatographic reader. (A) Peak values were recorded as the maximum value in interval b (Y_b), interval d (Y_d), or interval f (Y_f). The background values were calculated with the minimum value in interval a (Y_a), interval c (Y_c), interval e (Y_e), or interval g (Y_g). (B) Example of one positive sample and one negative sample. The small chart is the screen display of the immunochromatographic reader.

After incubation at room temperature for 10 min, the cassette was set in an immunochromatographic reader (Figure 1B).

The fluorescence intensity was measured by scanning the cassette at 100 μm intervals in an immunochromatographic reader with 365 nm laser. The measurement would be completed in 25 s, and the result would be directly displayed on the liquid crystal display panel of the reader. The measurement would be repeated thrice, and a median value was used to minimize the impact of extreme values. The final intensity data could optionally be exported as a Microsoft Excel file and saved on a local PC via USB connection.

To further improve the detection efficiency, a simplified background subtraction method was applied. The peak value was recorded as the maximum value in interval b (Y_b), interval d (Y_d) or interval f (Y_f). The background value was calculated with the minimum value in interval a (Y_a), interval c (Y_c), interval e (Y_e) or interval g (Y_g). For example, the average value of Y_a and Y_c was set as the background value of Y_b . And the final IgG value and IgM value were calculated by using the following formula (Figure 2).

$$Y_a = \min(Y_{31}, Y_{32}, \dots, Y_{60}); \quad Y_b = \max(Y_{61}, Y_{62}, \dots, Y_{90});$$

$$Y_c = \min(Y_{91}, Y_{92}, \dots, Y_{105}); \quad Y_d = \max(Y_{106}, Y_{107}, \dots, Y_{120});$$

$$Y_e = \min(Y_{121}, Y_{122}, \dots, Y_{140}); \quad Y_f = \max(Y_{141}, Y_{142}, \dots, Y_{160});$$

$$Y_g = \min(Y_{161}, Y_{162}, \dots, Y_{180})$$

$$C = Y_b - \text{mean}(Y_a, Y_c); \quad T1 = Y_d - \text{mean}(Y_c, Y_e);$$

$$T2 = Y_f - \text{mean}(Y_e, Y_g)$$

$$\text{IgG} = T1/C; \quad \text{IgM} = T2/C$$

GraphPad Prism ver. 5.0 was used for graphing. SPSS 20.0 was used for statistical analysis.

RESULTS AND DISCUSSION

SARS-CoV2 IgG/IgM rapid immunochromatographic assay (Serum/Plasma) is a solid phase immunochromatographic assay for the rapid, qualitative/semiquantitative, and differ-

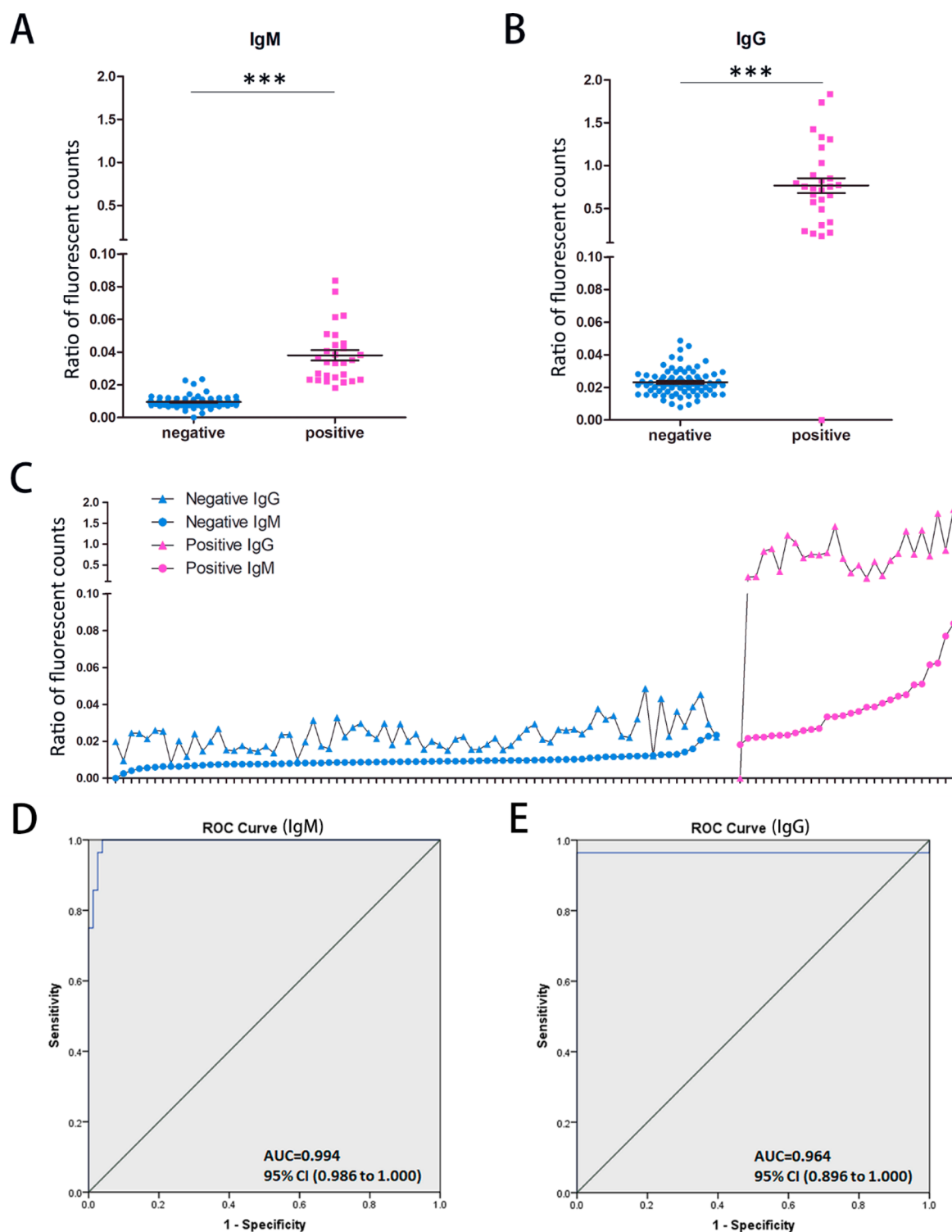


Figure 3. Fluorescent intensity of serum from healthy people and COVID-19 patients in the immunochromatographic assay. Scatterplot of IgM (A) and IgG (B). *** means $P < 0.0001$. Horizontal bars show the mean intensity. Comparison of IgM to IgG levels within the same individual (C). Fitted ROC curves of IgM (D) and IgG (E).

ent detection of IgG and IgM antibodies to SARS-CoV2 in human serum or plasma.

When a specimen followed by assay buffer is introduced into the sample well, IgM and/or IgG antibodies, if present, will bind to SARS-CoV2 conjugates making a complex of antigen and antibodies. This complex migrates through nitrocellulose membrane by capillary action from nitrocellulose. When the

complex meets the line of the corresponding immobilized antibody (anti-human IgM and/or anti-human IgG) the complex is trapped, and fluorescence can be detected showing a positive result. The fluorescence intensity can be used to quantitate the concentration of targeting IgM/IgG. Absence of fluorescence or low fluorescence indicates a negative result. The control line will also show strong fluorescence regardless

of the fluorescence intensity of the IgM and/or IgG lines. The absence of the fluorescence from the control line means that the test is invalid, and the specimen must be retested.

Figure 1C displays four testing results to explain the working mode of the cassette under UV lamp. The figure showed results from four different serum or plasma samples (one from a healthy person and three from patients): In cartridge b, no IgM and IgG (a health person); in cartridge c, low concentration of IgM and IgG (an early patient); in cartridge d, high concentration of IgM and IgG (an acute patient); in cartridge e, high concentration of IgG and no IgM (a convalescent patient) (Figure 1C).

SARS-CoV2 IgG/IgM rapid immunochromatographic assay was tested with a total of 28 positive and 77 negative serum or plasma samples. The results were exported from the immunochromatographic reader and analyzed on Microsoft Excel software. The following formulas were used for calculating the specificity and sensitivity rate:

$$\text{Specificity} = [\text{True negative}/(\text{False positive} + \text{True negative})] \times 100$$

$$\text{Sensitivity} = [\text{True positive}/(\text{False negative} + \text{True positive})] \times 100$$

The IgM value of negative samples ranged from 0 to 0.0234 (average = 0.0094; SD = 0.0035) and that of positive samples ranged from 0.0181 to 0.0839 (average = 0.0381; SD = 0.0169) ($P < 0.001$). The IgG value of negative samples ranged from 0.0079 to 0.0486 (average = 0.0231; SD = 0.0080) and that of positive samples ranged from 0 to 1.8328 (average = 0.7675; SD = 0.4633) ($P < 0.001$). The normal distribution curves of IgM and IgG were made from readings. The difference of IgG values between positive and negative samples was large enough to distinguish with the naked eye by using a UV lamp, but the difference of IgM values between positive and negative samples was too little to distinguish with the naked eye; the critical IgM value could only be distinguished by professional instruments. Based on the test data of serum or plasma from COVID-19 patients and healthy people, the sensitivity and specificity of the immunochromatographic assay were calculated as 98.72% and 100% (IgG), and 98.68% and 93.10% (IgM), respectively. Receiver operating characteristic (ROC) curve analysis showed AUC, 0.994; 95% CI, 0.986 to 1.000 for IgM, and AUC, 0.964; 95% CI, 0.896 to 1.000 for IgG (Figure 3). Since the test time of immunochromatographic assay was set to 10 min, the method was shown to be successful for rapid serodiagnosis of COVID-19.

The major finding of our clinical evaluation of the SARS-CoV2 IgG/IgM rapid immunochromatographic assay was that this rapid detection method solved the problem of rapid quantification of serum antibody. Since IgM is the earliest antibody produced by the human body after infection with the virus,^{15,19} it is the most valuable index for early clinical serodiagnosis of COVID-19. Nevertheless, IgM's output is lower than that of IgG, making the inspection more difficult. In our rapid detection assay, the IgM values of positive samples were obviously lower than that of IgG. Only professional equipment could distinguish the differences of the IgM value between positive and negative samples in some cases. Fluorescence immunochromatography solved the important defect of gold colloid technology, which is difficult to quantify

and was more sensitive and specific than the traditional colloidal gold immunochromatography. Therefore, the lanthanide, Eu (III) fluorescent microsphere based immunochromatography was suitable for SARS-CoV2 diagnosis.^{20–22}

Coronaviruses are RNA viruses, which can cause respiratory, enteric, hepatic, and neurologic diseases among humans, mammals, and birds. Up to the present day, there are seven coronavirus species; among them there are three strains, 2003 SARS-CoV, 2012 MERS-CoV, and 2019 SARS-CoV-2, which can cause serious respiratory and even fatal illness.^{3–5} SARS-CoV-2 belongs to the β coronavirus genus, just similar to SARS-CoV 2003 and MERS-CoV 2012. Its genome size is about 30 kilobases encoding several nonstructural and structural proteins. There are four kinds of main structural proteins include NP, spike protein, membrane protein, and envelope protein. Within these proteins, NP is a more valuable diagnostic candidate for the following reasons. NP has low polymorphism and high expression level in coronaviruses.^{23,24} The amino acid sequence of NP of SARS-CoV2 was just similar to another human infectious coronavirus (SARS-CoV), bat coronavirus and pangolin coronavirus, and that was different from another human infectious coronavirus such as MERS-CoV or other animal coronavirus with a similarity of amino acid sequence less than 50%. Previous study suggested that antibodies were generated during infection against the NP of SARS-CoV, the most abundantly expressed structural protein with high immunogenicity, and it was also highly prevalent in SARS-CoV patients. NP of SARS-CoV2 is more conservative when compared with S protein, but it is quite different from other human infectious coronaviruses except SARS-CoV. The recombinant NP had cross reactivity with antibodies from SARS-CoV and SARS-CoV2 patients by dot-blot, and the rapid immunochromatographic assay was also. The cross reaction with SARS virus antibody during the SARS-CoV2 epidemic probably would not hinder the application of the detection kit. Therefore, NP was used as the diagnostic antigen in this study.

In conclusion, an immunochromatographic assay using lanthanide, Eu (III) fluorescent microspheres with NP as capture antigen was useful for rapid serodiagnosis of COVID-19. We hope developing this antibody detection method by using fluorescent microspheres would apply to clinical medicine in this new coronavirus outbreak.

■ ASSOCIATED CONTENT

Supporting Information

The Supporting Information is available free of charge at <https://pubs.acs.org/doi/10.1021/acssensors.0c00927>.

Materials; supporting figure and supporting methods (PDF)

■ AUTHOR INFORMATION

Corresponding Authors

Xunjia Cheng – Department of Medical Microbiology and Parasitology, School of Basic Medical Sciences, Fudan University, Shanghai 200032, China; orcid.org/0000-0002-8851-6903; Email: xjcheng@shmu.edu.cn

Guodong Sui – Department of Environmental Science and Engineering, Fudan University, Shanghai 200438, China; orcid.org/0000-0002-6751-0852; Email: gsui@fudan.edu.cn

Authors

Meng Feng – Department of Medical Microbiology and Parasitology, School of Basic Medical Sciences, Fudan University, Shanghai 200032, China

Jun Chen – Department of Infectious Diseases and Immunology, Shanghai Public Health Clinical Center, Shanghai 201508, China

Jingna Xun – Department of Infectious Diseases and Immunology, Shanghai Public Health Clinical Center, Shanghai 201508, China

Ruixue Dai – Department of Environmental Science and Engineering, Fudan University, Shanghai 200438, China

Wang Zhao – Department of Environmental Science and Engineering, Fudan University, Shanghai 200438, China

Hongzhou Lu – Department of Infectious Diseases and Immunology, Shanghai Public Health Clinical Center, Shanghai 201508, China

Jin Xu – Division of Infection, Children's Hospital of Fudan University, Shanghai 201103, China

Li Chen – Department of Medical Microbiology and Parasitology, School of Basic Medical Sciences, Fudan University, Shanghai 200032, China

Complete contact information is available at:

<https://pubs.acs.org/10.1021/acssensors.0c00927>

Author Contributions

M.F., J.C., R.D., W.Z. conducted the experiments designed by X.C. and G.S. J.C., J.X., H.L., and J.X. performed assay test of clinical samples. M.F., X.C., G.S., and L.C. analyzed the data and wrote the manuscript. All authors read and approved the final manuscript. M.F. and J.C. contributed equally.

Notes

The authors declare no competing financial interest.

ACKNOWLEDGMENTS

This work was supported by the novel coronavirus research project of Fudan University (IDF101029) and National Key Research and Development Program of China (2018YFA0507304). We thanked the Novoprotein Technology Co., Ltd for its help in sample ordering and product integration.

REFERENCES

- (1) Wang, C.; Horby, P. W.; Hayden, F. G.; Gao, G. F. A novel coronavirus outbreak of global health concern. *Lancet* **2020**, *395*, 470–473.
- (2) Zhu, N.; Zhang, D.; Wang, W.; et al. A Novel Coronavirus from Patients with Pneumonia in China, 2019. *N. Engl. J. Med.* **2020**, *382*, 727.
- (3) Kuiken, T.; Fouchier, R. A.; Schutten, M.; Rimmelzwaan, G.; Amerongen, G.; Riel, D.; Laman, J.; Jong, T.; Doornum, G.; Lim, W.; Ling, A. E.; Chan, P. K.; Tam, J. S.; Zambon, M. C.; Gopal, R.; Drosten, C.; Werf, S.; Escriou, N.; Manuguerra, J. C.; Stöhr, K.; Peiris, J. S. M.; Osterhaus, A. D. Newly discovered coronavirus as the primary cause of severe acute respiratory syndrome. *Lancet* **2003**, *362*, 263–270.
- (4) World-Health-Organization; Update 49 - SARS case fatality ratio, incubation period. Available online: https://www.who.int/csr/sars/archive/2003_05_07a/en/.
- (5) World-Health-Organization; Middle East respiratory syndrome coronavirus (MERS-CoV). Available online: <https://www.who.int/emergencies/mers-cov/en/>.
- (6) Jin, Y. H.; Cai, L.; Cheng, Z. S.; Cheng, H.; Deng, T.; Fan, Y. P.; Fang, C.; Huang, D.; Huang, L. Q.; Huang, Q.; Han, Y.; Hu, B.; Hu,

F.; Li, B. H.; Li, Y. R.; Liang, K.; Lin, L. K.; Luo, L. S.; Ma, J.; Ma, L. L.; Peng, Z. Y.; Pan, Y. B.; Pan, Z. Y.; Ren, X. Q.; Sun, H. M.; Wang, Y.; Wang, Y. Y.; Weng, H.; Wei, C. J.; Wu, D. F.; Xia, J.; Xiong, Y.; Xu, H. B.; Yao, X. M.; Yuan, Y. F.; Ye, T. S.; Zhang, X. C.; Zhang, Y. W.; Zhang, Y. G.; Zhang, H. M.; Zhao, Y.; Zhao, M. J.; Zi, H.; Zeng, X. T.; Wang, Y. Y.; Wang, X. H. A rapid advice guideline for the diagnosis and treatment of 2019 novel coronavirus (COVID-19) infected pneumonia (standard version). *Mil. Med. Res.* **2020**, *7*, 4.

(7) Chu, C. M.; Leung, W. S.; Cheng, V. C.; Chan, K. H.; Lin, A. W.; Chan, V. L.; Lam, J. Y.; Chan, K. S.; Yuen, K. Y. Duration of RT-PCR positivity in severe acute respiratory syndrome. *Eur. Respir. J.* **2005**, *25*, 12–14.

(8) Zheng, Z.; Yao, Z.; Wu, K.; Zheng, J. The diagnosis of SARS-CoV2 pneumonia: a review of laboratory and radiological testing results. *J. Med. Virol.* **2020**, *28*, 1 DOI: 10.1002/jmv.26081.

(9) Gallagher, J. Are Coronavirus Tests Flawed? BBC News, www.bbc.com/news/health-51491763, 2020.

(10) Imai, K.; Tabata, S.; Ikeda, M.; Noguchi, S.; Kitagawa, Y.; Matuoka, M.; Miyoshi, K.; Tarumoto, N.; Sakai, J.; Ito, T.; Maesaki, S.; Tamura, K.; Maedac, T. Clinical evaluation of an immunochromatographic IgM/IgG antibody assay and chest computed tomography for the diagnosis of COVID-19. *J. Clin. Virol.* **2020**, *128*, 104393.

(11) Haveri, A.; Smura, T.; Kuivanen, S.; Österlund, P.; Hepojoki, J.; Ikonen, N.; Pitkääpaasi, M.; Blomqvist, S.; Rönkkö, E.; Kantele, A.; Strandin, T.; Kallio-Kokko, H.; Mannonen, L.; Lappalainen, M.; Broas, M.; Jiang, M.; Siira, L.; Salminen, M.; Puumalainen, T.; Sane, J.; Melin, M.; Vapalahti, O.; Savolainen-Kopra, C. Serological and molecular findings during SARS-CoV-2 infection: The first case study in Finland, January to February 2020. *Euro. Surveill.* **2020**, *25*, 2000266.

(12) Chen, Z.; Zhang, Z.; Zhai, X.; Li, Y.; Lin, L.; Zhao, H.; Bian, L.; Li, P.; Yu, L.; Wu, Y.; Lin, G. Rapid and sensitive detection of anti-SARS-CoV-2 IgG, using lanthanide-doped nanoparticles-based lateral flow immunoassay. *Anal. Chem.* **2020**, *92*, 7226–7231.

(13) Wan, Z. Y.; Zhang, X.; Yan, X. G. IFA in testing specific antibody of SARS coronavirus. *South China J. Prev. Med.* **2003**, *29*, 36–37.

(14) Che, X.; Di, B.; Zhao, G.; Wang, Y.; Qiu, L.; Hao, W.; Wang, M.; Qin, P.; Liu, Y.; Chan, K.; Cheng, V. C.; Yuen, K. A patient with asymptomatic severe acute respiratory syndrome (SARS) and antigenemia from the 2003–2004 community outbreak of SARS in Guangzhou, China. *Clin. Infect. Dis.* **2006**, *43*, e1–5.

(15) Zhang, G.; Nie, S.; Zhang, Z.; Zhang, Z. Longitudinal change of SARS-Cov2 antibodies in patients with COVID-19. *J. Infect. Dis.* **2020**, *222*, 183.

(16) Barbosa Junior, W. L.; Ramos de Araujo, P. S.; Dias de Andrade, L.; Aguiar Dos Santos, A. M.; Lopes da Silva, M. A.; Dantas-Torres, F.; Medeiros, Z. Rapid tests and the diagnosis of visceral leishmaniasis and human immunodeficiency virus/acquired immunodeficiency syndrome coinfection. *Am. J. Trop. Med. Hyg.* **2015**, *93*, 967–969.

(17) Janwan, P.; Intapan, P. M.; Yamasaki, H.; Yamasaki, H.; Rodpai, R.; Laummaunwai, P.; Thanchomngang, T.; Sanpool, O.; Kobayashi, K.; Takayama, K.; Kobayashi, Y.; Maleewong, W. Development and usefulness of an immunochromatographic device to detect antibodies for rapid diagnosis of human gnathostomiasis. *Parasites Vectors* **2016**, *9*, 14.

(18) Liu, J.; Shao, H.; Tao, Y.; Yang, B.; Qian, L.; Yang, X.; Cao, B.; Hu, G.; Tachibana, H.; Cheng, X. Production of an anti-severe acute respiratory syndrome (SARS) coronavirus human monoclonal antibody Fab fragment by using a combinatorial immunoglobulin gene library derived from patients who recovered from SARS. *Clin. Vaccine Immunol.* **2006**, *13*, 594–597.

(19) Peiris, J. S.; Chu, C. M.; Cheng, V. C.; Chan, K. S.; Hung, I. F.; Poon, L. L.; Law, K. L.; Tang, B. S.; Hon, T. Y.; Chan, C. S.; Chan, K. H.; Ng, J. S.; Zheng, B. J.; Ng, W. L.; Lai, R. W.; Guan, Y.; Yuen, K. Y. HKU/UCH SARS Study Group; Clinical progression and viral load in

a community outbreak of coronavirus-associated SARS pneumonia: a prospective study. *Lancet* **2003**, *361*, 1767–1772.

(20) Xie, Q. Y.; Wu, Y. H.; Xiong, Q. R.; Xu, H. Y.; Xiong, Y. H.; Liu, K.; Jin, Y.; Lai, W. H. Advantages of fluorescent microspheres compared with colloidal gold as a label in immunochromatographic lateral flow assays. *Biosens. Bioelectron.* **2014**, *54*, 262–265.

(21) Song, C.; Zhi, A.; Liu, Q.; Yang, J.; Jia, G.; Shervin, J.; Tang, L.; Hu, X.; Deng, R.; Xu, C.; Zhang, G. Rapid and sensitive detection of β -agonists using a portable fluorescence biosensor based on fluorescent nanosilica and a lateral flow test strip. *Biosens. Bioelectron.* **2013**, *50*, 62–65.

(22) Xu, W.; Chen, X.; Huang, X.; Yang, W.; Liu, C.; Lai, W.; Xu, H.; Xiong, Y. Ru(phen)₃(2+) doped silica nanoparticle based immunochromatographic strip for rapid quantitative detection of β -agonist residues in swine urine. *Talanta* **2013**, *114*, 160–166.

(23) Zhou, P.; Yang, X. L.; Wang, X. G.; Hu, B.; Zhang, L.; Zhang, W.; Si, H. R.; Zhu, Y.; Li, B.; Huang, C. L.; Chen, H. D.; Chen, J.; Luo, Y.; Guo, H.; Jiang, R. D.; Liu, M. Q.; Chen, Y.; Shen, X. R.; Wang, X.; Zheng, S. H.; Zhao, K.; Chen, Q. J.; Deng, F.; Liu, L. L.; Yan, B.; Zhan, F. X.; Wang, Y. Y.; Xiao, G. F.; Shi, Z. L. A pneumonia outbreak associated with a new coronavirus of probable bat origin. *Nature* **2020**, *579*, 270.

(24) Lu, R.; Zhao, X.; Li, J.; Niu, P.; Yang, B.; Wu, H.; Wang, W.; Song, H.; Huang, B.; Zhu, N.; Bi, Y.; Ma, X.; Zhan, F.; Wang, L.; Hu, T.; Zhou, H.; Hu, Z.; Zhou, W.; Zhao, L.; Chen, J.; Meng, Y.; Wang, J.; Lin, Y.; Yuan, J.; Xie, Z.; Ma, J.; Liu, W. J.; Wang, D.; Xu, W.; Holmes, E. C.; Gao, G. F.; Wu, G.; Chen, W.; Shi, W.; Tan, W. Genomic characterization and epidemiology of 2019 novel coronavirus: Implications for virus origins and receptor binding. *Lancet* **2020**, *6736*, 565.